HHS Public Access

Author manuscript

Neurosci Lett. Author manuscript; available in PMC 2017 April 21.

Published in final edited form as:

Neurosci Lett. 2016 February 26; 615: 21–27. doi:10.1016/j.neulet.2016.01.014.

Depressed basal hypothalamic neuronal activity in type-1 diabetic mice is correlated with proinflammatory secretion of HMBG1

Jeffrey S. Thinschmidt[1], **Luis M. Colon Perez**[2], **Marcelo Febo**[2], **Sergio Caballero**[1], **Michael A. King**[1], **Fletcher A. White**[3], and **Maria B. Grant, MD.**[4,†]

[1]Department of Pharmacology and Therapeutics, University of Florida, Gainesville, FL, USA

[2]Department of Psychiatry, University of Florida, Gainesville, Florida, FL, USA

[3]Department of Anesthesia, Indiana University School of Medicine, Indianapolis, IN, USA

[4]Eugene and Marilyn Glick Eye Institute, Department of Ophthalmology, Indiana University School of Medicine, Indianapolis, IN, USA

Abstract

We recently found indicators of hypothalamic inflammation and neurodegeneration linked to the loss of neuroprotective factors including insulin-like growth factor (IGF-1) and IGF binding protein-2 (IGFBP-3) in mice made diabetic using streptozotocin (STZ). In the current work, a genetic model of type-1 diabetes ($Ins2^{Akita}$ mouse) was used to evaluate changes in neuronal activity and concomitant changes in the proinflammatory mediator high-mobility group box-1 (HMBG1). We found basal hypothalamic neuronal activity as indicated by manganese-enhanced magnetic resonance imaging (MEMRI) was significantly decreased in 8 month old, but not 2 month old $Ins2^{Akita}$ diabetic mice compared to controls. In tissue from the same animals we evaluated the expression of HMBG1 using immunohistochemistry and confocal microscopy. We found decreased HMBG1 nuclear localization in the paraventricular nucleus of the hypothalamus (PVN) in 8 month old, but not 2 month old diabetic animals indicating nuclear release of the protein consistent with an inflammatory state. Adjacent thalamic regions showed little change in HMBG1 nuclear localization and neuronal activity as a result of diabetes. This work extends our previous findings demonstrating changes consistent with hypothalamic neuroinflammation in STZ treated animals, and shows active inflammatory processes are correlated with changes in basal hypothalamic neuronal activity in $Ins2^{Akita}$ mice.

Keywords

Akita; HMBG1; MEMRI; diabetes; neuroinflammation

[†]Corresponding author at: Eugene and Marilyn Glick Eye Institute, Department of Ophthalmology, Department of Cellular and Integrative Physiology, Indiana University School of Medicine, 980 W. Walnut St R3-C41 Indianapolis, IN 46202, Tel.: +1 (317) 274 2628.

INTRODUCTION

Peripheral and central nervous system (CNS) pathology can result from chronic hyperglycemia [50] and neuroinflammation has been implicated in the pathogenesis of diabetes associated neuropathy and CNS disease [64]. We recently found CNS inflammation in mice made diabetic using STZ, as bone marrow-derived hypothalamic microglia/macrophages were activated and found at higher densities compared to controls [27]. Also, infiltration of $CD45^{+/}CCR2^{+}/GR\text{-}1^{+}/Iba\text{-}1^{+}$ bone marrow-derived monocytes were attenuated with the anti-inflammatory agent minocycline, which crosses the blood-brain barrier. We suggested that targeting central inflammation may facilitate the management of microvascular complications in diabetes as we found a shift in hematopoiesis toward generation of monocytes and a loss of sympathetic efferent connections from the brain to the bone marrow [27]. More recently, we found other evidence for hypothalamic inflammation in STZ treated mice, including a reduction in the expression of CD39 in microglia and blood vessels, and increased $MMP\text{-}2^{+}$ expression in astrocytes, both of which were reversed with minocycline treatment [26].

HMBG1 is an intranuclear protein that is proinflammatory when passively released into the extracellular environment by necrotic cells [18]. Also, it can be actively secreted by macrophages or monocytes via translocation from the nucleus to the cytoplasm. Once secreted, HMBG1 acts as a cytokine signaling at the receptor for advanced glycated end-products (RAGE) and at Toll-like receptors (TLR2/4) producing inflammatory responses involving the production of chemoattraction of stem cells, cytokines, induction of vascular adhesion molecules, and impaired function of epithelial cells [18]. HMBG1 mediated inflammatory processes have been shown in many conditions including lung inflammation [2], experimental sepsis [62], and arthritis [49]. Elevated glucose can produce release of HMBG1 from the nucleus to the cytosol [57] and raise HMBG1 levels in both endothelial cell cultures [45] and the plasma of diabetic patients [14]. Consistent with this, increases in HMBG1 levels have been shown in diabetes [66] and are specifically implicated in inflammatory processes involved in diabetic retinopathy [3–5, 24, 44]. A role for HMBG1 in brain inflammation has been shown in ischemic damage [11], epileptic seizure [42], traumatic brain injury [35, 58], and neuropathic pain [6, 7, 19]. However, no studies to our knowledge have evaluated changes in HMBG1 in the brain resulting from diabetes, but it appears likely that inflammatory processes associated with hyperglycemia may produce such changes. Further, changes in neuronal activity may be initiated by the release of HMBG1. This is supported by experiments showing the ability of HMBG1 to affect neuronal activity in dissociated neurons (DRGs) following activation of TLR4, and HMBG1's actions at the RAGE receptor [7, 19, 28, 42].

Neurocognitive deficits are found in patients with type-1 diabetes [29] and these are associated with structural changes in the white matter of the brain [36, 59]. Subcortical damage to the brain resulting from type-1 diabetes has been demonstrated by studies showing changes in synaptic plasticity [34] and direct damage to neurons in the hypothalamus and hippocampus [33, 39]. However, there is a paucity of information regarding how diabetes may affect regional basal neuronal activity. Metabolic physiology

can be studied with the use of functional neuroimaging using manganese (Mn^{2+}) which enters cells via voltage-gated calcium channels and produces increased MRI signal intensity in regions with augmented neuronal excitation [53]. Specific activation of hypothalamic nuclei as measured by MEMRI has been demonstrated with alterations in feeding [37] and administration of gut hormones [47]. Thus, MEMRI appears ideal to study hypothalamic neuronal activity in the disturbed metabolic environment of diabetes.

In the hypothalamus, the paraventricular nucleus (PVN) is a key relay in the control of sympathetic nervous activity, and it receives and integrates inputs from the brainstem and forebrain. Sympathetic outflow to peripheral organs is modulated via PVN efferents to the rostral ventrolateral medulla (RVLM) and the intermediolateral (IML) column of the spinal cord [1, 8, 13, 20, 21, 25, 46]. The PVN receives direct and indirect neural and blood-borne information (glucose, leptin, ghrelin, and insulin) about fluid homeostasis, satiety, metabolic state, and digestive system activity, processes this information, and directly contributes to coordinated autonomic output to the viscera. Importantly, it appears that PVN neurons can become vulnerable to the chronic metabolic disturbances associated with diabetes.

In the current work we investigated basal neuronal activity in the PVN and surrounding hypothalamic regions using MEMRI in hyperglycemic $Ins2^{Akita}$ mice and hypothesized that differences relative to control animals would be correlated with local inflammatory processes, specifically translocation of HMBG1 from the nucleus to the cytoplasm.

MATERIALS AND METHODS

Subjects

$Ins2^{Akita}$ mice are heterozygous for the insulin-2 spontaneous mutation. The animals exhibit hyperglycemia 3–4 weeks after birth. Thus, these animals appear as an ideal Type-1 model and eliminate potential confounds (e.g. neurotoxicity) associated with streptozotocin. Male $Ins2^{Akita}$ mice and controls with identical backgrounds (C57BL/6J) (~2 months old) were obtained from the Jackson Laboratory (Bar Harbor, ME) and housed in a temperature and humidity-controlled vivarium (12 h light-dark cycle, lights off at 19:00 h). Food and water were available *ad libitum* in the home cages. Blood glucose was tested weekly in $Ins2^{Akita}$ mice and insulin was not administered as animals maintained healthy weights and body condition scores throughout the housing period. Blood glucose was consistently above 500 mg/dl in all $Ins2^{Akita}$ mice. The experimental protocols were approved by the UF Institutional Animal Care and Use Committee and complied with the Guide for the Care and Use of Laboratory Animals.

$MnCl_2$ injections

In order to map basal brain activity in $Ins2^{Akita}$ mice and non-diabetic controls, manganese (II) chloride tetrahydrate (St. Louis, MO, USA) was dissolved in ddH_2O and injected (IP: 70 mg/kg) 24hrs prior to MRI scanning. Following injections the animals were returned to their home cage and imaged the following day.

Manganese enhanced MRI

Animals previously injected with $MnCl_2$ were anesthetized with 3–4% isoflurane in air for 60 s. The isoflurane concentration was maintained between 2 and 3% during the setup of the animal for imaging and was kept between 1 and 1.5% during image acquisition. Mice were placed prone on a custom-made plastic bed with a respiratory pad and warm water bed system (SA Instruments, Stony Brook, NY, USA). The core body temperature was maintained at 37–38 °C. The respiratory rate was monitored continuously during data acquisition and isoflurane levels were adjusted to maintain breathing rate at approximately 30 respiratory strokes per min. Images were collected on a 4.7 Tesla Magnex Scientific MR scanner controlled by Agilent Technologies VnmrJ 3.1 console software. A quadrature transmit/receive coil tuned to 200 MHz was used for B_1 excitation and signal detection (AIRMRI, LLC, Holden, MA). Images were acquired using a T_1 -weighted spin echo pulse sequence with the following parameters: repetition time (TR) = 407.4 ms, echo time (TE) = 14.8 ms, number of averages (NA) = 30, in plane resolution = 117 microns^2 (0.117mm^2), slice thickness = 0.8 mm, 20 slices. Total scan time per mouse was 52 min. 13 seconds.

Data processing and statistical analysis

Images were processed and analyzed as previously reported [48]. Mn^{2+} accumulation in active neurons produces signal intensity increases in T_1 images. However, as this is a non-quantitative approach to measure activity and because there is scan-to-scan intensity variation independent of Mn^{2+}, we normalized images based on their individual variance [48]. Using this normalization approach, we have observed significant differences between Mn^{2+} administered and non-treated rodents, where surpassing a normalized threshold value of 1 indicates increased activity associated with Mn^{2+} administration. Image processing was carried out using itk SNAP (http://www.itksnap.org) and image math scripts available on FSL (*fslmaths* http://www.fmrib.ox.ac.uk/fsl/). Scans were aligned with a segmented atlas of the adult mouse brain using an automated affine linear registration tool from FSL [31]. Each scan was converted to a z value map through a voxel-wise normalization procedure. The mean signal intensity across the entire extracted brain volume ($\bar{x}$) was subtracted from each voxel (xi) and then divided by the variance (σ). A pre-set threshold of $z \geq 1$ was selected based on *a priori* observation of individual datasets and a close inspection of their intensity distribution histograms. All voxels with z score values below this threshold were set to zero. Thus, the voxels exceeding the threshold value of $z \geq 1$ were considered in our statistical analysis as having higher signal intensities (quantified as mean signal intensity and as the number of voxels above a z value of 1). Mean normalized signal intensity values for each ROI were compared using an unpaired two-tailed t-test (homoscedastic variances, $\alpha \leq 0.05$).

Immunohistochemical procedures for HMBG1 colocalization experiments

Following fMRI scans animals were kept anesthetized and overdosed with 100mg/kg pentobarbital (i.p.). The chest cavity was opened and transcardial perfusion was performed using a 30ml syringe; first with 20ml of PBS followed by 20ml of 4% formaldehyde in PBS. Brains were removed and stored in fixative overnight and then switched to 20% sucrose in PBS and stored at 4°C. Sectioning was performed on a cryostat set to yield 25 μm coronal sections. Sections were mounted on glass slides and stored at −80°C until processed.

Slides were washed 3x with PBS to remove excess embedding media and incubated in an antigen retrieval citrate-based solution (BioGenex, Fremont, CA) for 30 min. Slides were blocked with 10% NGS for 20 min, washed again with PBS, and incubated in primary antibody (Anti-HMBG1, ab79823, 1:100 (Abcam, Cambridge, MA)) overnight at 4°C. The next day slides were washed and transferred to secondary antibody (goat anti-rabbit, 1:500) conjugated with Alexa488 (Invitrogen–Molecular Probes, Carlsbad, CA) for 30 min. Slides were washed again with PBS and coverslips were set with Vectashield® containing DAPI for nuclear staining (H-1000 + DAPI, Burlingame, CA).

Confocal microscopy and image analysis

The PVN was identified in each section and digital image captures were made using a laser scanning confocal microscope (Leica TCS SP2, Leica Microsystems, Buffalo Grove, IL). Z-series captures (1 mm z-depth) were made through the entire section thickness, yielding approximately 15–25 images per stack. A minimum of three random 63x fields centered in the PVN were captured for each animal. The fields were acquired from the most central aspect of the nucleus and included both magnocellular and parvocellular regions. Also, control regions adjacent (dorsal) to the PVN were captured in each section. Software-assisted color thresholding and density slicing was used to measure the area of fluorescence for each channel used in the spatially calibrated images (ImageJ, NIH Research Service Branch, http://rsb.info.nih.gov/ij/index.html). Co-localization of markers was accomplished in software prior to morphometric analysis (Intensity Correlation Analysis plugin, MBF Plugin Collection, http://rsbweb.nih.gov/ij/plugins/mbf-collection.html), and was calculated as a function of total voxel volume within the field and normalized to control values [30, 38]. Images representing colocalized signal were subjected to threshold analysis for determination of total area of positive colocalization. Values for area were summed for the entire stack. Summed areas for each stack were then averaged for each condition. Values for each stack were then averaged for a single animal, thus providing a single value for each animal. Those values were then used to determine differences between the various groups by t-test for the null hypothesis, with known variance. A $P \leq 0.05$ was considered significant. Graphs were completed using GraphPad Prism and Microsoft Excel.

RESULTS

Manganese enhanced MRI

Averaged basal neuronal activity maps ($n = 5$) for each condition are shown in Figure 1A. There was an apparent overall reduction in hypothalamic activity found in 8 month old $Ins2^{Akita}$ mice (Figure 1A, lower right panel) compared to 8 month old controls (Figure 1A, lower left panel) with little obvious difference between 2 month old $Ins2^{Akita}$ mice and controls (Figure 1A, upper panels). Two ROIs were constructed for analyses which included the entire hypothalamus and the PVN region. Quantification of signal intensity for these ROIs are shown in Figure 1B & C. Relative signal intensities (see methods) for the entire hypothalamus were reduced in aged 8 month old $Ins2^{Akita}$ mice compared to controls (1.53 ± 0.04 vs 1.64 ± 0.09, $n = 5$) and in 2 month old $Ins2^{Akita}$ mice compared to controls (1.55 ± 0.05 vs 1.63 ± 0.09, $n = 5$) but these differences were not statistically significant. Further analyses of ROIs containing only the PVN region showed a statistically significant reduction

in signal intensity ($p < 0.05$) in aged 8 month old Ins2^{Akita} mice compared to controls (1.44 ± 0.05 vs 1.77 ± 0.01, $n = 5$) but no differences between 2 month old Ins2^{Akita} mice compared to controls (1.68 ± 0.06 vs 1.65 ± 0.2, $n = 5$) (Figure 1C). There were no significant differences between any groups using ROIs adjacent to the hypothalamus in the periventricular thalamic region (data not shown).

Translocation of HMBG1 to cytoplasm in PVN

HMBG1 (green) and DAPI (blue) were easily detected in all tissue sections (Figure 2A). Image stacks were acquired for each sample and processed as outlined above (see methods). Intensity correlation plots were generated depicting the probability of colocalization of HMBG1 and DAPI (Figure 2B) and the total volume of positive nuclear localization was determined throughout the entire stack. For control (thalamic) regions and the PVN, the total colocalized volume was normalized to the average volume of the control mice at each age. We found a significant ($p < 0.02$) reduction in colocalization of DAPI and HMBG1 in 8 month old Ins2^{Akita} mice ($n = 4$) compared to controls ($n = 4$) (0.49 ± 0.10 vs 1 ± 0.15) in the PVN (Figure 2C,D,E). However, no significant differences were found in adjacent thalamic control regions in the same sections (1.17 ± 0.23 vs 1 ± 0.1) (Figure 2E). In addition, no significant differences in the volume of colocalization were found between 2 month old Ins2^{Akita} mice ($n = 4$) and controls ($n = 4$) in the PVN (0.79 ± 0.13 vs 1 ± 0.28) or adjacent thalamic control regions in the same sections (0.76 ± 0.05 vs 1 ± 0.25) Figure 2E.

DISCUSSION

We found a significant reduction in basal PVN hypothalamic neuronal activity in 8 month old Ins2^{Akita} mice using MEMRI. Significant changes in neuronal activity were not found in adjacent control regions or in 2 month old Ins2^{Akita} mice. There was a significant reduction in colocalization of HMBG1 with DAPI in the PVN of 8 month old Ins2^{Akita} mice, indicating HMBG1 was released from nuclei to cytosols consistent with an inflammatory state. This was not observed in adjacent control regions or in 2 month old Ins2^{Akita} mice which endured less hyperglycemia.

fMRI studies have shown oral glucose produces inhibition in the human hypothalamus [54] including the PVN region [43], and peripheral glucose injections produce hypothalamic inhibition in the rat [41]. However, little attention has been paid to the long-term effects of chronic hyperglycemia on regional neuronal activity, and to our knowledge, this is the first report showing a relatively widespread depression in basal neuronal activity in the hypothalamus of diabetic mice. On the cellular level, others have shown high glucose can increase c-Fos expression in rat PVN neurons [10, 17] and high glucose diets can produce increases in intracellular Ca^{2+} in PVN neurons in mice [22]. However, differences between brain activity measured by fMRI and markers of activity (c-Fos) in single neurons have been documented elsewhere [16, 55, 63] and show that these methods can yield conflicting results. Also, chronic and acute high glucose should not be expected to produce similar effects on neuronal activity.

Magnocellular neurons in the PVN and SON respond to hyperosmolality by increasing their production of vasopressin [34]. Early in diabetes these neurons are chronically activated [32]

and show an upregulation of c-Fos [67] and NMDA receptor expression [40]. However, in the present report basal PVN neuronal activity was not significantly different in 2 month old Ins2^{Akita} mice compared to controls. Differences between mice treated with STZ and Ins2^{Akita} mice may account for this, also the ability to detect such changes may not be possible using MEMRI. The PVN contains GABAergic interneurons and preautonomic neurons which are also affected shortly after STZ treatment, showing diminished, rather than increased excitation [23]. Future studies using electrophysiological methods with Ins2^{Akita} mice may be able to resolve whether our results involve generalized effects on PVN neuronal activity or if these changes are specific to any particular cell type. Finally, increases in PVN neuronal excitation in response to glucose may be acutely adaptive, but chronic activation may produce detrimental effects. Our previous findings [26] and other work [15, 40] showing neuronal degeneration following long-term diabetes are consistent with this observation. Thus, it is possible that reduced basal hypothalamic activity in the present report could have resulted from the loss of neurons over time. Future studies evaluating neuronal densities in Ins2^{Akita} mice may be able to resolve this.

We have proposed that CNS inflammation produces increases in sympathetic drive altering peripheral nerve activity in the bone marrow and shifting hematopoiesis toward generation of monocytes, ultimately producing microvascular complications [27]. It has been demonstrated that sympathetic nerve activity increases following glucose intake after meals [9] and glucose injected into the PVN produces increases in sympathetic drive [52]. However, the long-term effects of chronic hyperglycemia on sympathetic activity are unknown. It appears possible that depressed hypothalamic activity found in the current report may produce changes in sympathetic output, either increasing or decreasing sympathetic drive based on whether inhibitory or excitatory inputs are most affected. Future studies using simultaneous peripheral nerve and brain activity measurements could determine this relationship.

HMBG1 is released passively by necrotic cells and actively by macrophages and some populations of injured neurons indicating it can be an early initiator or late promotor of inflammation [18, 19, 42]. The data in the current report are consistent with other work indicating HMBG1 is eventually released from the cytosol in diabetes, producing extracellular concentrations above levels found in controls [14, 45, 66]. Circulating HMBG1 can increase serum TNF levels *in vivo* [18] and may act like a cytokine, inducing proinflammatory responses in macrophages and monocytes. To our knowledge there are no reports showing changes in inflammatory cytokines in Ins2^{Akita} mice mouse brains but such changes have been found in the heart [12] and retina [65]. We [27] and others [40] have shown that microglia are activated and found at higher densities in STZ treated animals and a role for HMBG1 has been indicated in diabetic pain [51], diabetic heart disease [56] and diabetic retinopathy [3–5, 24, 44]. Adding to these findings, our data demonstrate the potential for HMBG1 mediated brain inflammation in diabetes, and suggest that end organ complications resulting from diabetes may be initiated or exacerbated by changes in CNS activity produced by inflammation. Thus, targeting CNS inflammation may prove useful for treating peripheral organ damage seen in diabetes.

It is known that inflammatory reactions occur in response to neuronal hyperactivity [60]. Also, inflammatory insults can produce increases in neuronal activation [61]. Though the present findings show depressed basal neuronal activity is correlated with HMBG1 translocation to the cytosol, it is quite possible that long term inflammatory conditions involving HMBG1 could also affect neuronal activity and that changes in neuronal activity could produce HMBG1 mediated inflammation [7, 19, 42]. Our previous findings [26, 27] and the present report indicate an inflammatory state in the hypothalamus of diabetic animals involving changes in HMBG1, activation of microglia, depressed hypothalamic neuronal activity, and neuronal atrophy. Future work will concentrate on the sequence in which the above occur, if these processes are causally linked to one another, and an examination comparing inflammatory markers and neuronal activity in STZ-treated, $Ins2^{Akita}$, and control mice.

Acknowledgments

This work was supported by grants R01EY007739, R01EY012601, and R0110170 to MBG. R01DK100905 and I01BX001860 to FAW. MF was supported by NIG grant DA019946, DA038009 and funding from the McKnight Brain Institute of the University of Florida. This work was conducted in part at the University of Florida McKnight Brain Institute National High Magnetic Field Laboratory's AMRIS Facility, which is supported by National Science Foundation Cooperative Agreement No. DMR-1157490 and the State of Florida.

References

1. Abboud FM, Harwani SC, Chapleau MW. Autonomic neural regulation of the immune system: implications for hypertension and cardiovascular disease. Hypertension. 2012; 59:755–762. [PubMed: 22331383]
2. Abraham E, Arcaroli J, Carmody A, Wang H, Tracey KJ. HMG-1 as a mediator of acute lung inflammation. Journal of immunology. 2000; 165:2950–2954.
3. Abu El-Asrar AM, Mohammad G, Nawaz MI, Siddiquei MM. High-Mobility Group Box-1 Modulates the Expression of Inflammatory and Angiogenic Signaling Pathways in Diabetic Retina. Current eye research. 2014:1–12.
4. Abu El-Asrar AM, Nawaz MI, Kangave D, Abouammoh M, Mohammad G. High-mobility group box-1 and endothelial cell angiogenic markers in the vitreous from patients with proliferative diabetic retinopathy. Mediators of inflammation. 2012; 2012:697489. [PubMed: 23118492]
5. Abu El-Asrar AM, Nawaz MI, Siddiquei MM, Al-Kharashi AS, Kangave D, Mohammad G. High-mobility group box-1 induces decreased brain-derived neurotrophic factor-mediated neuroprotection in the diabetic retina. Mediators of inflammation. 2013; 2013:863036. [PubMed: 23766563]
6. Agalave NM, Larsson M, Abdelmoaty S, Su J, Baharpoor A, Lundback P, Palmblad K, Andersson U, Harris H, Svensson CI. Spinal HMGB1 induces TLR4-mediated long-lasting hypersensitivity and glial activation and regulates pain-like behavior in experimental arthritis. Pain. 2014; 155:1802–1813. [PubMed: 24954167]
7. Allette YM, Due MR, Wilson SM, Feldman P, Ripsch MS, Khanna R, White FA. Identification of a functional interaction of HMGB1 with Receptor for Advanced Glycation End-products in a model of neuropathic pain. Brain, behavior and immunity. 2014; 42:169–177.
8. Benarroch EE, Schmeichel AM, Low PA, Boeve BF, Sandroni P, Parisi JE. Involvement of medullary regions controlling sympathetic output in Lewy body disease. Brain: a journal of neurology. 2005; 128:338–344. [PubMed: 15634729]
9. Berne C, Fagius J, Niklasson F. Sympathetic response to oral carbohydrate administration. Evidence from microelectrode nerve recordings. The Journal of clinical investigation. 1989; 84:1403–1409. [PubMed: 2681266]

10. Carrasco M, Portillo F, Larsen PJ, Vallo JJ. Insulin and glucose administration stimulates Fos expression in neurones of the paraventricular nucleus that project to autonomic preganglionic structures. Journal of neuroendocrinology. 2001; 13:339–346. [PubMed: 11264721]
11. C. Centers for Disease. Tuberculosis outbreak on Standing Rock Sioux Reservation--North Dakota and South Dakota, 1987–1990. MMWR. Morbidity and mortality weekly report. 1991; 40:204–207. [PubMed: 1900567]
12. Chavali V, Tyagi SC, Mishra PK. Differential expression of dicer, miRNAs, and inflammatory markers in diabetic Ins2+/− Akita hearts. Cell Biochem Biophys. 2014; 68:25–35. [PubMed: 23797610]
13. Dampney RA, Horiuchi J. Functional organisation of central cardiovascular pathways: studies using c-fos gene expression. Progress in neurobiology. 2003; 71:359–384. [PubMed: 14757116]
14. Dandona P, Ghanim H, Green K, Sia CL, Abuaysheh S, Kuhadiya N, Batra M, Dhindsa S, Chaudhuri A. Insulin infusion suppresses while glucose infusion induces Toll-like receptors and high-mobility group-B1 protein expression in mononuclear cells of type 1 diabetes patients. American journal of physiology Endocrinology and metabolism. 2013; 304:E810–818. [PubMed: 23403945]
15. Dheen ST, Tay SS, Wong WC. Ultrastructural changes in the hypothalamic supraoptic nucleus of the streptozotocin-induced diabetic rat. Journal of anatomy. 1994; 184(Pt 3):615–623. [PubMed: 7928649]
16. Dodd GT, Williams SR, Luckman SM. Functional magnetic resonance imaging and c-Fos mapping in rats following a glucoprivic dose of 2-deoxy-D-glucose. Journal of neurochemistry. 2010; 113:1123–1132. [PubMed: 20236391]
17. Dunn-Meynell AA, Govek E, Levin BE. Intracarotid glucose selectively increases Fos-like immunoreactivity in paraventricular, ventromedial and dorsomedial nuclei neurons. Brain research. 1997; 748:100–106. [PubMed: 9067450]
18. Erlandsson Harris H, Andersson U. Mini-review: The nuclear protein HMGB1 as a proinflammatory mediator. European journal of immunology. 2004; 34:1503–1512. [PubMed: 15162419]
19. Feldman P, Due MR, Ripsch MS, Khanna R, White FA. The persistent release of HMGB1 contributes to tactile hyperalgesia in a rodent model of neuropathic pain. J Neuroinflammation. 2012; 9:180. [PubMed: 22824385]
20. Ferguson AV, Latchford KJ, Samson WK. The paraventricular nucleus of the hypothalamus - a potential target for integrative treatment of autonomic dysfunction. Expert opinion on therapeutic targets. 2008; 12:717–727. [PubMed: 18479218]
21. Fisher JP, Paton JF. The sympathetic nervous system and blood pressure in humans: implications for hypertension. Journal of human hypertension. 2012; 26:463–475. [PubMed: 21734720]
22. Gantulga D, Maejima Y, Nakata M, Yada T. Glucose and insulin induce Ca2+ signaling in nesfatin-1 neurons in the hypothalamic paraventricular nucleus. Biochemical and biophysical research communications. 2012; 420:811–815. [PubMed: 22465118]
23. Gao H, Miyata K, Bhaskaran MD, Derbenev AV, Zsombok A. Transient receptor potential vanilloid type 1-dependent regulation of liver-related neurons in the paraventricular nucleus of the hypothalamus diminished in the type 1 diabetic mouse. Diabetes. 2012; 61:1381–1390. [PubMed: 22492526]
24. Gong Y, Jin X, Wang QS, Wei SH, Hou BK, Li HY, Zhang MN, Li ZH. The involvement of high mobility group 1 cytokine and phospholipases A2 in diabetic retinopathy. Lipids in health and disease. 2014; 13:156. [PubMed: 25292258]
25. Guyenet PG. The sympathetic control of blood pressure. Nature reviews Neuroscience. 2006; 7:335–346. [PubMed: 16760914]
26. Hu P, Thinschmidt JS, Caballero S, Adamson S, Cole L, Chan-Ling T, Grant MB. Loss of survival factors and activation of inflammatory cascades in brain sympathetic centers in type 1 diabetic mice. American journal of physiology Endocrinology and metabolism. 2015; 308:E688–698. [PubMed: 25714673]
27. Hu P, Thinschmidt JS, Yan Y, Hazra S, Bhatwadekar A, Caballero S, Salazar T, Miyan JA, Li W, Derbenev A, Zsombok A, Tikhonenko M, Dominguez JM 2nd, McGorray SP, Saban DR, Boulton

ME, Busik JV, Raizada MK, Chan-Ling T, Grant MB. CNS inflammation and bone marrow neuropathy in type 1 diabetes. The American journal of pathology. 2013; 183:1608–1620. [PubMed: 24160325]

28. Hua XY, Chen P, Fox A, Myers RR. Involvement of cytokines in lipopolysaccharide-induced facilitation of CGRP release from capsaicin-sensitive nerves in the trachea: studies with interleukin-1beta and tumor necrosis factor-alpha. The Journal of neuroscience: the official journal of the Society for Neuroscience. 1996; 16:4742–4748. [PubMed: 8764661]
29. Jacobson AM, Musen G, Ryan CM, Silvers N, Cleary P, Waberski B, Burwood A, Weinger K, Bayless M, Dahms W, Harth J. Diabetes, Control Complications Trial/Epidemiology of Diabetes, Interventions Complications Study Research, Group: Long-term effect of diabetes and its treatment on cognitive function. The New England journal of medicine. 2007; 356:1842–1852. [PubMed: 17476010]
30. Jaskolski F, Mulle C, Manzoni OJ. An automated method to quantify and visualize colocalized fluorescent signals. Journal of neuroscience methods. 2005; 146:42–49. [PubMed: 15935219]
31. Jenkinson M, Bannister P, Brady M, Smith S. Improved optimization for the robust and accurate linear registration and motion correction of brain images. NeuroImage. 2002; 17:825–841. [PubMed: 12377157]
32. Klein JP, Craner MJ, Cummins TR, Black JA, Waxman SG. Sodium channel expression in hypothalamic osmosensitive neurons in experimental diabetes. Neuroreport. 2002; 13:1481–1484. [PubMed: 12167778]
33. Klein JP, Hains BC, Craner MJ, Black JA, Waxman SG. Apoptosis of vasopressinergic hypothalamic neurons in chronic diabetes mellitus. Neurobiology of disease. 2004; 15:221–228. [PubMed: 15006692]
34. Klein JP, Waxman SG. The brain in diabetes: molecular changes in neurons and their implications for end-organ damage. The Lancet Neurology. 2003; 2:548–554. [PubMed: 12941577]
35. Kobori N, Clifton GL, Dash P. Altered expression of novel genes in the cerebral cortex following experimental brain injury. Brain research Molecular brain research. 2002; 104:148–158. [PubMed: 12225869]
36. Kodl CT, Franc DT, Rao JP, Anderson FS, Thomas W, Mueller BA, Lim KO, Seaquist ER. Diffusion tensor imaging identifies deficits in white matter microstructure in subjects with type 1 diabetes that correlate with reduced neurocognitive function. Diabetes. 2008; 57:3083–3089. [PubMed: 18694971]
37. Kuo YT, Herlihy AH, So PW, Bhakoo KK, Bell JD. In vivo measurements of T1 relaxation times in mouse brain associated with different modes of systemic administration of manganese chloride. Journal of magnetic resonance imaging: JMRI. 2005; 21:334–339. [PubMed: 15779025]
38. Li Q, Lau A, Morris TJ, Guo L, Fordyce CB, Stanley EF. A syntaxin 1, Galpha(o), and N-type calcium channel complex at a presynaptic nerve terminal: analysis by quantitative immunocolocalization. The Journal of neuroscience: the official journal of the Society for Neuroscience. 2004; 24:4070–4081. [PubMed: 15102922]
39. Li ZG, Zhang W, Grunberger G, Sima AA. Hippocampal neuronal apoptosis in type 1 diabetes. Brain research. 2002; 946:221–231. [PubMed: 12137925]
40. Luo Y, Kaur C, Ling EA. Neuronal and glial response in the rat hypothalamus-neurohypophysis complex with streptozotocin-induced diabetes. Brain research. 2002; 925:42–54. [PubMed: 11755899]
41. Mahankali S, Liu Y, Pu Y, Wang J, Chen CW, Fox PT, Gao JH. In vivo fMRI demonstration of hypothalamic function following intraperitoneal glucose administration in a rat model. Magnetic resonance in medicine. 2000; 43:155–159. [PubMed: 10642744]
42. Maroso M, Balosso S, Ravizza T, Liu J, Aronica E, Iyer AM, Rossetti C, Molteni M, Casalgrandi M, Manfredi AA, Bianchi ME, Vezzani A. Toll-like receptor 4 and high-mobility group box-1 are involved in ictogenesis and can be targeted to reduce seizures. Nat Med. 2010; 16:413–419. [PubMed: 20348922]
43. Matsuda M, Liu Y, Mahankali S, Pu Y, Mahankali A, Wang J, DeFronzo RA, Fox PT, Gao JH. Altered hypothalamic function in response to glucose ingestion in obese humans. Diabetes. 1999; 48:1801–1806. [PubMed: 10480611]

44. Mohammad G, Siddiquei MM, Othman A, Al-Shabrawey M, Abu El-Asrar AM. High-mobility group box-1 protein activates inflammatory signaling pathway components and disrupts retinal vascular-barrier in the diabetic retina. Experimental eye research. 2013; 107:101–109. [PubMed: 23261684]
45. Mudaliar H, Pollock C, Ma J, Wu H, Chadban S, Panchapakesan U. The role of TLR2 and 4-mediated inflammatory pathways in endothelial cells exposed to high glucose. PloS one. 2014; 9:e108844. [PubMed: 25303153]
46. Osborn JW, Collister JP, Guzman P. Effect of peripheral sympathetic nerve dysfunction on salt sensitivity of arterial pressure. Clinical and experimental pharmacology & physiology. 2008; 35:273–279. [PubMed: 17973927]
47. Parkinson JR, Chaudhri OB, Kuo YT, Field BC, Herlihy AH, Dhillo WS, Ghatei MA, Bloom SR, Bell JD. Differential patterns of neuronal activation in the brainstem and hypothalamus following peripheral injection of GLP-1, oxyntomodulin and lithium chloride in mice detected by manganese-enhanced magnetic resonance imaging (MEMRI). NeuroImage. 2009; 44:1022–1031. [PubMed: 18983926]
48. Perez PD, Hall G, Kimura T, Ren Y, Bailey RM, Lewis J, Febo M, Sahara N. In vivo functional brain mapping in a conditional mouse model of human tauopathy (tauP301L) reveals reduced neural activity in memory formation structures. Molecular neurodegeneration. 2013; 8:9. [PubMed: 23379588]
49. Pullerits R, Jonsson IM, Verdrengh M, Bokarewa M, Andersson U, Erlandsson-Harris H, Tarkowski A. High mobility group box chromosomal protein 1, a DNA binding cytokine, induces arthritis. Arthritis and rheumatism. 2003; 48:1693–1700. [PubMed: 12794838]
50. Reijmer YD, van den Berg E, Ruis C, Kappelle LJ, Biessels GJ. Cognitive dysfunction in patients with type 2 diabetes. Diabetes/metabolism research and reviews. 2010; 26:507–519. [PubMed: 20799243]
51. Ren PC, Zhang Y, Zhang XD, An LJ, Lv HG, He J, Gao CJ, Sun XD. High-mobility group box 1 contributes to mechanical allodynia and spinal astrocytic activation in a mouse model of type 2 diabetes. Brain research bulletin. 2012; 88:332–337. [PubMed: 22459482]
52. Sakaguchi T, Bray GA. Sympathetic activity following paraventricular injections of glucose and insulin. Brain research bulletin. 1988; 21:25–29. [PubMed: 3064881]
53. Silva AC, Lee JH, Aoki I, Koretsky AP. Manganese-enhanced magnetic resonance imaging (MEMRI): methodological and practical considerations. NMR in biomedicine. 2004; 17:532–543. [PubMed: 15617052]
54. Smeets PA, de Graaf C, Stafleu A, van Osch MJ, van der Grond J. Functional magnetic resonance imaging of human hypothalamic responses to sweet taste and calories. The American journal of clinical nutrition. 2005; 82:1011–1016. [PubMed: 16280432]
55. Stark JA, Davies KE, Williams SR, Luckman SM. Functional magnetic resonance imaging and c-Fos mapping in rats following an anorectic dose of m-chlorophenylpiperazine. NeuroImage. 2006; 31:1228–1237. [PubMed: 16549369]
56. Volz HC, Seidel C, Laohachewin D, Kaya Z, Muller OJ, Pleger ST, Lasitschka F, Bianchi ME, Remppis A, Bierhaus A, Katus HA, Andrassy M. HMGB1: the missing link between diabetes mellitus and heart failure. Basic research in cardiology. 2010; 105:805–820. [PubMed: 20703492]
57. Wang Y, Shan J, Yang W, Zheng H, Xue S. High mobility group box 1 (HMGB1) mediates high-glucose-induced calcification in vascular smooth muscle cells of saphenous veins. Inflammation. 2013; 36:1592–1604. [PubMed: 23928875]
58. Weber DJ, Gracon AS, Ripsch MS, Fisher AJ, Cheon BM, Pandya PH, Vittal R, Capitano ML, Kim Y, Allette YM, Riley AA, McCarthy BP, Territo PR, Hutchins GD, Broxmeyer HE, Sandusky GE, White FA, Wilkes DS. The HMGB1-RAGE axis mediates traumatic brain injury-induced pulmonary dysfunction in lung transplantation. Sci Transl Med. 2014; 6:252ra124.
59. Wessels AM, Rombouts SA, Remijnse PL, Boom Y, Scheltens P, Barkhof F, Heine RJ, Snoek FJ. Cognitive performance in type 1 diabetes patients is associated with cerebral white matter volume. Diabetologia. 2007; 50:1763–1769. [PubMed: 17546438]
60. Xanthos DN, Sandkuhler J. Neurogenic neuroinflammation: inflammatory CNS reactions in response to neuronal activity. Nature reviews Neuroscience. 2014; 15:43–53. [PubMed: 24281245]

61. Xia Y, Krukoff TL. Differential neuronal activation in the hypothalamic paraventricular nucleus and autonomic/neuroendocrine responses to I.C.V. endotoxin. Neuroscience. 2003; 121:219–231. [PubMed: 12946713]

62. Yang H, Ochani M, Li J, Qiang X, Tanovic M, Harris HE, Susarla SM, Ulloa L, Wang H, DiRaimo R, Czura CJ, Wang H, Roth J, Warren HS, Fink MP, Fenton MJ, Andersson U, Tracey KJ. Reversing established sepsis with antagonists of endogenous high-mobility group box 1. Proceedings of the National Academy of Sciences of the United States of America. 2004; 101:296–301. [PubMed: 14695889]

63. Yang PF, Chen YY, Chen DY, Hu JW, Chen JH, Yen CT. Comparison of fMRI BOLD response patterns by electrical stimulation of the ventroposterior complex and medial thalamus of the rat. PloS one. 2013; 8:e66821. [PubMed: 23826146]

64. Yates KF, Sweat V, Yau PL, Turchiano MM, Convit A. Impact of metabolic syndrome on cognition and brain: a selected review of the literature. Arteriosclerosis, thrombosis and vascular biology. 2012; 32:2060–2067.

65. Zetterqvist AV, Blanco F, Ohman J, Kotova O, Berglund LM, de Frutos Garcia S, Al-Naemi R, Wigren M, McGuire PG, Gonzalez Bosc LV, Gomez MF. Nuclear factor of activated T cells is activated in the endothelium of retinal microvessels in diabetic mice. J Diabetes Res. 2015; 2015:428473. [PubMed: 25918731]

66. Zhao D, Wang Y, Tang K, Xu Y. Increased serum HMGB1 related with HbA1c in coronary artery disease with type 2 diabetes mellitus. International journal of cardiology. 2013; 168:1559–1560. [PubMed: 23336955]

67. Zheng H, Li YF, Weiss M, Mayhan WG, Patel KP. Neuronal expression of fos protein in the forebrain of diabetic rats. Brain research. 2002; 956:268–275. [PubMed: 12445695]

Highlights

- Hypothalamic neuronal activity is reduced following 8 months of Type-1 diabetes in mice.
- Basal neuronal activity is reduced in the paraventricular nucleus (PVN) following 8 months of Type-1 diabetes in mice.
- Nuclear localization of HMBG1 is reduced in the paraventricular nucleus (PVN) of the hypothalamus following 8 months of Type-1 diabetes in mice.
- Reduced nuclear localization of HMBG1 is correlated with a reduction in basal neuronal activity in the hypothalamus following 8 months of Type-1 diabetes in mice.

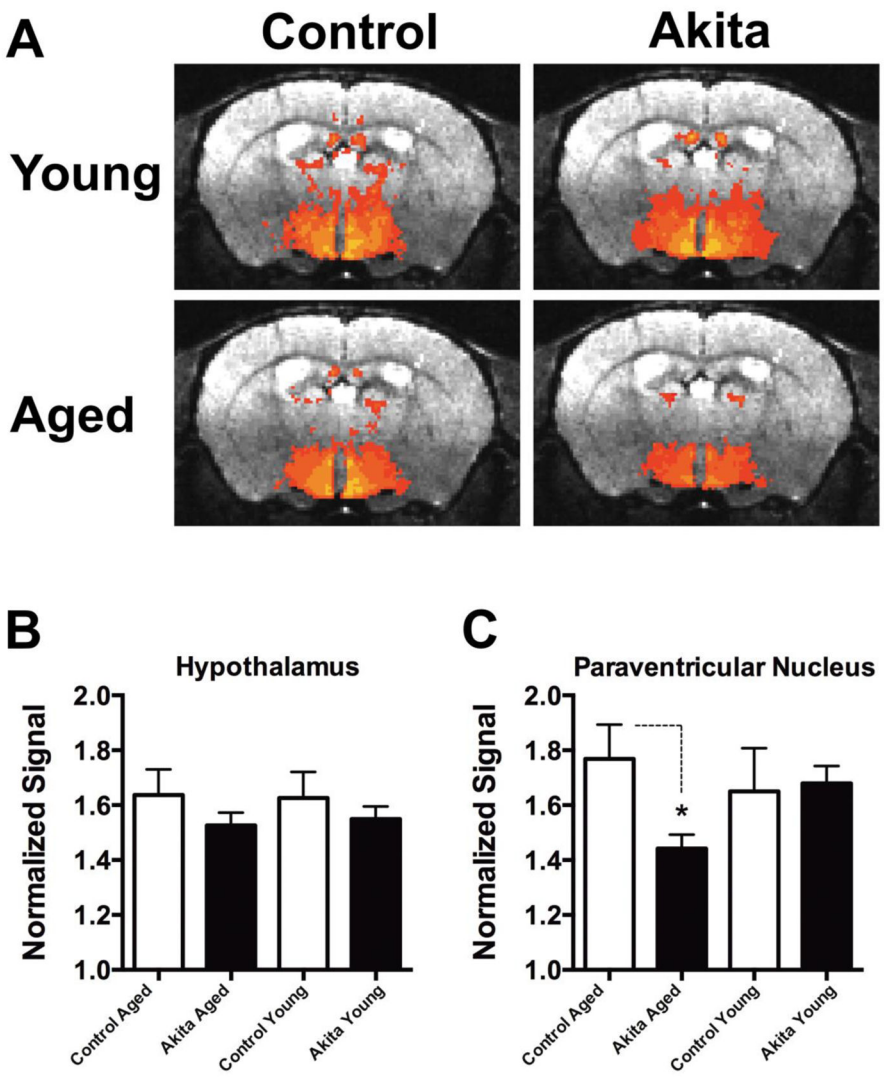

Figure 1. Basal hypothalamic neuronal activity is depressed in 8 month old Ins2^{Akita} mice

A) Averaged signal intensity maps (MEMRI) plotted on real brain atlas transverse sections in the central hypothalamus (PVN region). **Upper row:** averaged signal intensity maps from 2 month old Ins2^{Akita} mice (right), and 2 month old controls (left) showing little differences in most regions. **Lower row:** averaged signal intensity maps from 8 month old Ins2^{Akita} mice (right) and 8 month old controls (left) showing relative hypothalamic and PVN depression in Ins2^{Akita} mice. **B)** Bar chart showing quantification of normalized signal intensity for the entire hypothalamus and the PVN region **(C)** in all 4 experimental conditions.

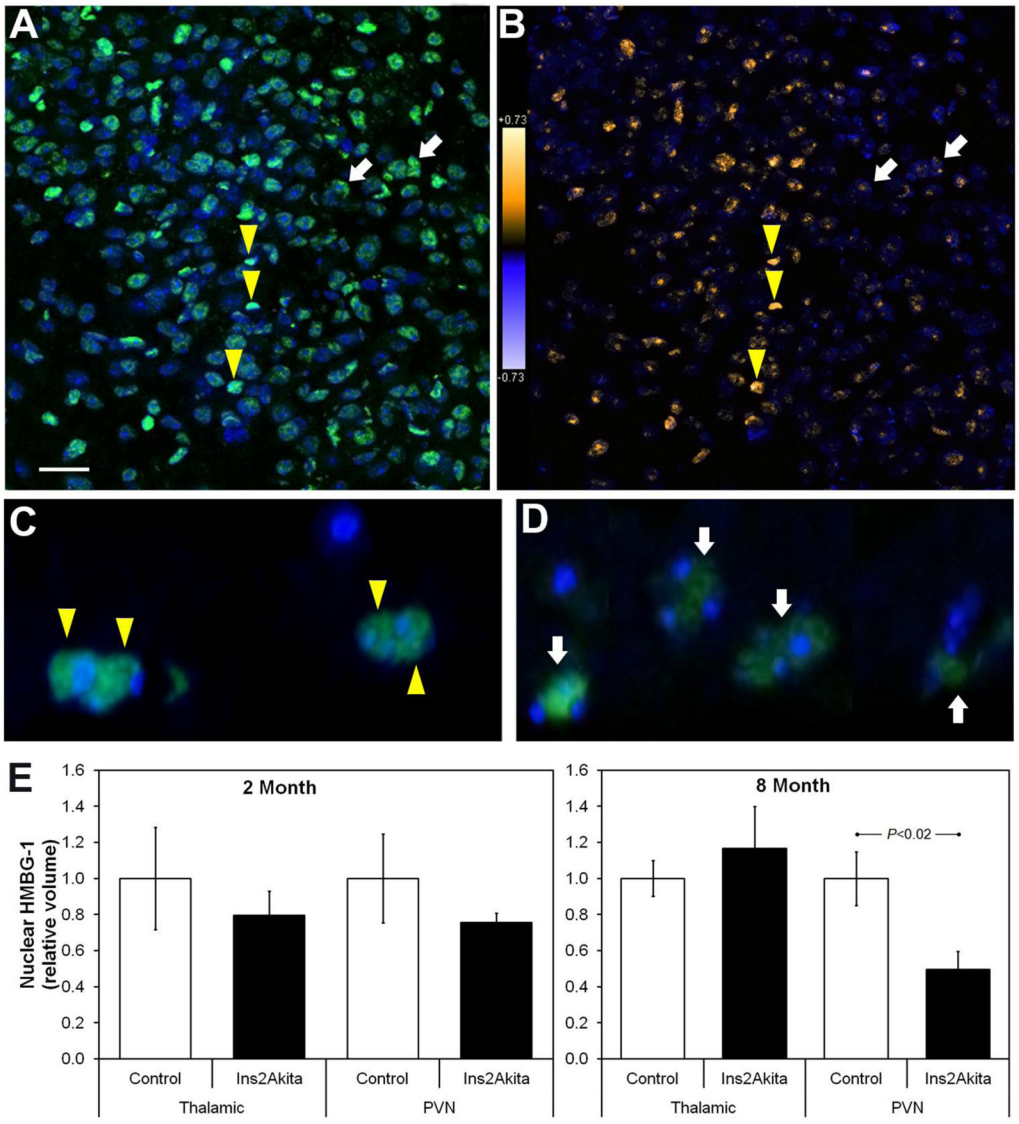

Figure 2. HMBG1 translocates from nucleus to cytoplasm with extended hyperglycemia – in the PVN of Ins2^{Akita} mice

(**A**) *En face* laser confocal microscopy image of a representative PVN region from a control mouse brain showing detection of nuclear (DAPI, blue) and HMBG1 (Alexa 488, green) fluorescence. (**B**) The same field as in (A) is shown after Intensity Correlation Analysis to determine the probability of colocalization. The analysis assigns warmer colors (yellows) to a high probability of colocalization and cooler colors to lower probability, allowing visualization of nuclear versus cytoplasmic HMBG1. The white arrows in (A–D) indicate typical cells with strong HMBG1 signal but low nuclear localization, while the yellow triangles show cells with strong nuclear HMBG1 localization. (**C & D**) Confocal microscopy depth projections of ~20 1μm sections of PVN regions. Aged-matched control (**C**) and 8-month diabetic Ins2Akita mice (**D**) illustrate HMBG1 nuclear localization and translocation at 100X. (**E**) Summary of quantitative volumetric morphometry measuring the

degree of nuclear HMBG1. A significant reduction in nuclear HMBG1 was observed in the PVN of $Ins2^{Akita}$ mice after 8 months of diabetes. Scale bar: 25μm (A & B).